FISEVIER

Contents lists available at ScienceDirect

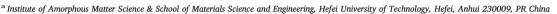
Computational Materials Science

journal homepage: www.elsevier.com/locate/commatsci



Embedded atom method potentials for Ce-Ni binary alloy

Yawei Lei^a, Xiaorui Sun^a, Rulong Zhou^{b,*}, Bo Zhang^{a,*}



^b School of Materials Science and Engineering, Hefei University of Technology, Hefei, Anhui 230009, PR China



ARTICLE INFO

Keywords: Embedded-atom-method (EAM) potential CeNi alloy Metallic glass

ABSTRACT

A new embedded-atom method (EAM) potential of Ce-Ni has been constructed based on the experimental and first-principles data with a variety of physical properties. The potential accurately reproduces the equilibrium lattice constant, cohesive energy, vacancy and interstitial formation energy, elastic constants, phonon dispersion and radial distribution functions of liquid amorphous structures of the alloys. With this potential, we investigated the glass forming ability and dynamic behavior of a deep-eutectic liquid $Ce_{80}Ni_{20}$. The simulated results of $Ce_{80}Ni_{20}$ metallic glass shows good agreement with related experimental data eg. the glass transition temperature and self-diffusion constant of Ni.

1. Introduction

Cerium and Ce-based compounds have drawn a lot of attention because of their fascinating properties. Due to the easier transition between the localized and itinerant states of the 4f electron, Ce exhibits a remarkable isostructural (fcc to fcc) phase transition from the ferromagnetic γ -Ce phase to the paramagnetic α -Ce phase under compression [1].

Cerium-based compounds also have unique characters due to the 4f electron. For example, pressure-induced superconductivity has been reported in CeIn₃, CePd₂Si₂ and CeCu₂Ga₂ [2]; CeAl₃ and CeCu₆ are heavy-fermion Kondo lattice compounds without any long-range magnetic order [3,4], and the cubic CeB₆ and CeAl₂ are Kondo lattice compounds that order magnetically at low temperature [5,6]. CeNi appears a pressure-induced first-order volume-collapse phase transition, because of the fluctuation of the charge states of the Ce atoms between Ce³⁺ and Ce⁴⁺. So CeNi is a typical model to study the mechanisms of phase transition caused by the f-electron instability and strong electron correlations [7].

Ce-based bulk metallic glasses (BMGs) also possess fascinating properties such as small elastic moduli, exceptionally low glass-transition temperature close to room temperature and excellent glass forming ability (GFA), etc. [8–10]. Hence, Ce-based BMGs were developed to study glass transition, plastic molding, slow dynamics [11] and glass-forming mechanism [12] in the glassy alloys, especially for $Ce_{80}Ni_{20}$ which is a deep eutectic system. However, although $Ce_{80}Ni_{20}$ compounds are expected to possess good glass-forming ability, Meyer et al. have shown that the synthesis of glassy $Ce_{80}Ni_{20}$ alloy by splat

quenching and melt spinning is unsuccessful [13]. To know the reason of this discrepancy between the fact and the expectation, it is needed to study the microstructural changes during the quenching and melt process.

Limited by the computer capacity, *ab initio* molecular dynamics simulation is incapable of simulating the kinetic processes involving lager model size and long simulation time. However classical molecular dynamics is possible to simulate structures with millions of atoms in reasonable time with classical effective potential. Therefore obtaining an effective potential for classical molecular dynamics is essential. In this paper we use force matching method proposed by Ercolessi and Adams [14] to develop an analytical embedded-atom method potential for Ce-Ni alloy. The potential is fitted to the calculated forces, energies and stresses of various structures from experiment data and *ab initio* MD simulations [15,16]. The open source program *potfit* [17] has developed as a flexible implementation of the force matching method.

To test the accuracy of our EAM potential, we compared the results calculated with the fitted EAM potential with those obtained from the density-functional theory (DFT) [18] calculations and experimental data. High consistence between the results of EAM potential and those from DFT calculations or experiments enabled us to use this potential to study the glass formation process and dynamic behavior of $Ce_{80}Ni_{20}$ melt

E-mail address: rlzhou@hfut.edu.cn (R. Zhou).

^{*} Corresponding authors.

2. Methodology

2.1. EAM potential

The total energy of an atomic system within Embedded-atom method [19,20] is represented as the following formula:

$$E_{tot} = \frac{1}{2} \sum_{i,j} \phi(n_{ij}) + \sum_{i} F(n_{i})$$
 (1)

and
$$n_i = \sum_{i} \rho(r_{ij})$$
 (2)

where $\phi(r_{ij})$ is a pair-wise potential function depending only on the distance (r_{ij}) of atom i and atom j. $F(n_i)$ is the embedding function that represents the energy required to place an atom into the electron cloud of density n_i , which is the sum of the contributions $\rho(r_{ij})$ from all the neighboring atoms.

For the pair-wise potential function, the Morse potential was adopted, which can be written as:

$$\phi(r) = \psi\left(\frac{r - r_c}{h}\right) D_e \{\left(1 - e^{-\alpha(r - r_e)}\right)^2 - 1\}$$
(3)

where the three parameters D_e , α and r_e describe the depth of the potential minimum, the width of the potential minimum and the equilibrium distance, respectively.

And, the function ψ is a cutoff function, which is defined as

$$\psi(x) = \begin{cases} \frac{x^4}{1+x^4}, & x < 0\\ 0, & x \geqslant 0 \end{cases}$$
 (4)

The parameters r and h in formula (3) describe the cutoff radius and the smoothing of the potential, respectively. The cutoff function guarantees that the potential functions, as well as their derivatives up to the second order, approach zero smoothly at the cutoff distance r_c .

As for the transfer function $\rho(r)$, we used an oscillating transfer function [21],

$$\rho(r) = \psi\left(\frac{r - r_c}{h}\right) \frac{1 + a_1 \cos(\kappa r) + a_2 \sin(\kappa r)}{r^{\beta}}$$
(5)

where the parameters a_1 and a_2 determine the amplitude of the oscillations, and κ is the wave vector and β controls the decay.

For the embedding function F(n), we chose the Johnson function [22] which is given by

$$F(n) = F_0[1 - q \ln n] n^q + F_1 n \tag{6}$$

 F_0 , F_1 and q are constants that we have to fit. $n = \rho_i/\rho_0$. ρ_0 is the equilibrium density. In this paper we use $\rho_0 = 1$.

For Ce-Ni binary system, the number of free parameters of our potential model is 23 with 7 potential functions (pair-wise functions for Ce-Ce, Ce-Ni and Ni-Ni, transfer functions for Ce and Ni, and embedding functions for Ce and Ni), and every pair and transfer function has one additional parameter h for the cutoff function ψ . The cutoff radius r_c is kept fixed at 7 Å.

2.2. Computational method

We used the Vienna Ab-initio Simulation Package (VASP) [23,24] to perform force and energy calculations using projector augmented wave (PAW) [25] potentials within the generalized gradient approximation (GGA) [26] with high precision. All the simulation supercells contain 96–128 atoms. A plane-wave cutoff energy of 400 eV was used along with $2 \times 2 \times 2$ Monkhorst–Pack k-point meshes[15]. Classical MD calculations were performed using the Large-scale Atomic/Molecular Massively Parallel Simulator (LAMMPS) code [27]. All force-matching was performed using the POTFIT package, which has previously been used to optimize tabulated pair and EAM potentials. The fitting error

defined through a least-squares function formed from the differences of the EAM and DFT (and experiment) values:

$$Z = Z_F + Z_C \tag{7}$$

 Z_F is related to the difference between the EAM and *ab initio* forces calculated for N_{α} atoms listed in the fitting database:

$$Z_F = \sum_{i=1}^{N_{\alpha}} \sum_{\alpha = x, y, z} W_i \frac{(F_{i\alpha}^{EAM} - F_{i\alpha}^{DFT})^2}{(F_{i\alpha}^{DFT})^2 + \varepsilon_i}$$
(8)

 $F_{i\alpha}$ is the α th component of the force on atom i, W_i is the weight associated with each force, and ε_i is a small value that helping us to avoid extremely small denominators.

 Z_C gives the fitting errors for energy and stress values:

$$Z_C = \sum_{i=1}^{N_C} W_i \frac{(A_i^{EAM} - A_i^{DFT})^2}{(A_i^{DFT})^2 + \varepsilon_i}$$
(9)

where N_C is the number of energies or stress tensor components for fitting, and A_i is the value of energy or stress.

3. Results and discussion

3.1. Error

We select 116 atomic configurations including 76 low-energy crystalline structures of pure Ni and various Ce-Ni compounds and 40 highly activated configurations (e.g. 14 structures with point defects, 24 structures with liquid phases, 2 structures with metallic glasses quenched at different cooling rates). The pure Ce crystalline structures are not included in our fitting database because there are two isostructure phases which are hard to be correctly described simultaneously by using density functional method. So, fitting including pure Ce phase can lead to large errors. However, this potential is mainly designed for simulating Ce-Ni binary systems, so the absence of pure Ce phases in the database will have little influence on the accuracy of this potential for Ce-Ni binary systems.

The root mean square (RMS) errors for forces, energies, and stresses are listed in Table 1. As seen, the RMS errors of the forces, energies and stresses are all smaller than the values reported in reference [28], which indicates that our fitting reaches a good accuracy. A graphical representation of the difference of energies, stresses and forces calculated by EAM potential and *ab initio* are shown in Fig. 1. As seen clearly, the maximum error between the EAM energy and *ab initio* energy is less than 25 meV/atom, and the average error is only 5.1 meV/atom. The average errors of stress and force are 90 bar and 168 meV/Å per configuration, respectively. All these results indicate that the results of the fitted EAM potential are in good consistence with the *ab initio* calculations. The profiles of the functions of our EAM potential are shown in Fig. 2.

We point out that although the RMS errors and average errors are very small, it is not enough to judge the quality and transferability of the fitted potential. Further comparison of various properties calculated using the fitted potential and the *ab initio* method is needed.

Table 1
Root mean square errors after the optimization for forces (in meV/Å), energies (in meV/atom), and stresses (in kPa).

RMS errors for	
Forces (meV/Å)	196.48
Energies (meV/atom)	6.99
Stresses (kPa)	39.00

Download English Version:

https://daneshyari.com/en/article/7957289

Download Persian Version:

https://daneshyari.com/article/7957289

Daneshyari.com